Volume 12 Number 2, 2018
doi: 10.25923/w4k8-a710

Quarterly

Editor: Manik Bali, ESSIC UMD

Newsletter–Summer 2018 Issue

CMA • CNES • EUMETSAT • IMD • ISRO • JAXA • JMA • KMA • NASA • NIST • NOAA • ROSCOSMOS . ROSHYDROMET • USGS • WMO

In This Issue

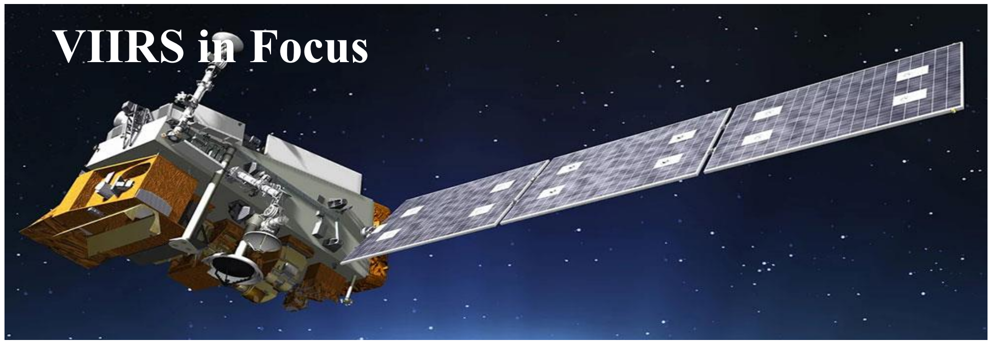

Image Above shows SNPP in orbit (Courtesy: NASA/NOAA)

GSICS recommends SNPP-VIIRS as the VIS/NIR calibration reference

By Dave Doelling (NASA), Chair GSICS VIS/NIR Subgroup

The GSICS VIS/NIR subgroup has officially recommended that SNPP-VIIRS be the VIS/NIR calibration reference sensor to radiometrically scale and to monitor the stability of current operational sensors. It was recommended to select the VIIRS spectral channel that best matches the target sensor. For example, the MODIS band 1 (0.65µm) spectral response function resembles the VIIRS I1 band more than the M5 band. The recommendations were agreed upon during the GSICS VIS/NIR web meeting held on July 5, 2018. The NOAA VIIRS IDPS L1B Version 2 (V2) dataset is the recommended calibrated VIIRS dataset. V2 is not available at the NOAA CLASS archive (www.class.noaa.gov) as it will take a year or two to reprocess the NPP VIIRS record. Changyong Cao, the NOAA VIIRS calibration lead, presented the VIIRS calibration improvements and invites any feedback regarding the VIIRS calibration effort. V2 mitigated the M1-M4 band calibration drifts contained in the V0 nominal calibrated dataset. GSICS will coordinate with NOAA to provide the calibration community with VIIRS L1B V2 granules over desert, DCC, SNO and other specific sites upon request, hopefully by this Fall. NASA-Langley will provide the GEO domain VIIRS DCC reference response, in the same manner as the Aqua-MODIS DCC reference response. The NOAA V2 calibration activities will be documented in order to provide the calibration community with a reference and calibration uncertainty. Both the MODIS and VIIRS instrument absolute calibrations based on the solar diffusers are reflectance based. To obtain radiance from the reflectance observations, a solar spectra is used. It must be noted, that the L1B MODIS, NPP-VIIRS, and NOAA-20, use the MCST, MODTRAN, and Thuillier solar spectra respectively.

doi: 10.25923/w4k8-a710
GSICS Quarterly: Winter Issue 2018 Volume 12, No. 2, 2018

Given the nature of sensor ageing and the corresponding incremental calibration improvements, the reference imagers will need to be reprocessed in order to incorporate the latest calibration improvements. Given the volume of data, the reprocessing effort could take years. Providing the remote sensing community up to date calibration in a timely manner is challenging in the current processing and archiving environment. During the NOAA STAR JPSS 2018 annual conference, a splinter group meeting organized by Changyong Cao was held on August 28, 2018, to discuss VIIRS calibration. David Doelling was invited to bring up any concerns that GSICS had regarding the VIIRS calibration, which are mentioned in this paragraph. The following suggestion were made. The first is to provide the calibration community calibrated granules over specific Earth targets, such as deserts, DCC, Dome-C, and SNO targets. Second, Andy Heidinger (NOAA) suggested that a full record of subsetted granules could be reprocessed quickly, since the data volume is much smaller when only every 20th pixels is processed. Third it was mentioned that the (raw) VIIRS RDR data is only one tenth of the L1B datasets. This could allow the user to process on their own computing systems the VIIRS RDR data and apply the latest calibration module. It is possible that the NOAA archive could provide V2 calibrated granules, which are processed upon request from the raw VIIRS RDR data, rather than distributing the reprocessed L1B archived dataset. This on-demand processing and other reprocessing details are discussed in the third article (Uprety et al) in this issue.

Discuss the Article

Performance of NOAA-20 VIIRS reflective solar bands revealed

By Junqiang Sun, NOAA

The NOAA-20 Visible Infrared Imaging Radiometer Suite (VIIRS) was launched into operation on November 18, 2017, and successfully obtained its first visible / reflective imagery on December 13, 2017. The flurry of post-launch activities that ensued includes establishing the on-orbit calibration operations and analyses that are to be carried out throughout the entire lifetime of the mission.

Among its suite of 22 bands, VIIRS contains 14 reflective solar bands (RSBs) along with a single panchromatic day/night band covering the spectral range of 0.41 to 2.25 μm. The RSBs are regularly calibrated and updated on orbit by using the onboard solar diffuser (SD) and solar diffuser stability monitor (SDSM). But the complete calibration pipeline requires several sets of fixed functions that must first be derived during the initial period of on-orbit operation [1]. One set is the bidirectional reflectance factors (BRFs) characterizing the reflectance of the SD in the two directions – from the SD to the SDSM and from the SD to the Rotation Telescope Assembly (RTA)which directs light to the RSBs. The second set is the vignetting function (VF) that characterizes the transmission screen in front of the SD port, or the SD Screen (SDS). The third set is the VFs that characterize the transmission screen in front of the sun-view (SV) port for the eight SDSM detectors. The SD BRFs, SDS VF and SVS VFs were measured prelaunch but need to be validated and improved from the on-orbit yaw measurements that were carried out on 25-26 January 2018 over 15 orbits. The accuracy of these fixed functions are not of trivial matter, and inaccuracy in them can introduce errors, along with artificial seasonal variations into the calibrated sensor data records (SDRs) and their associated science products.

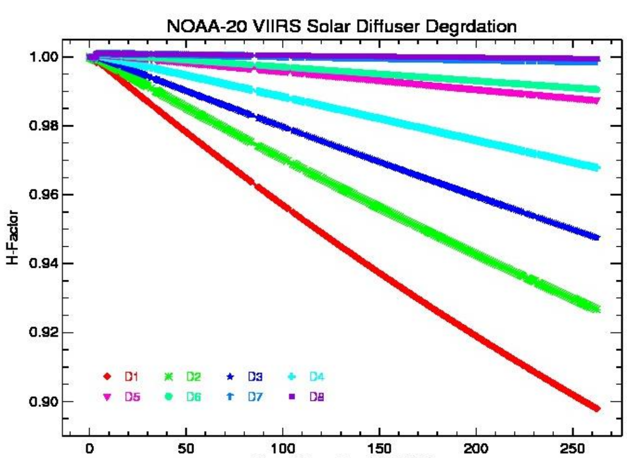

Figure 1. NOAA-20 VIIRS SD degradation (or H-factors).

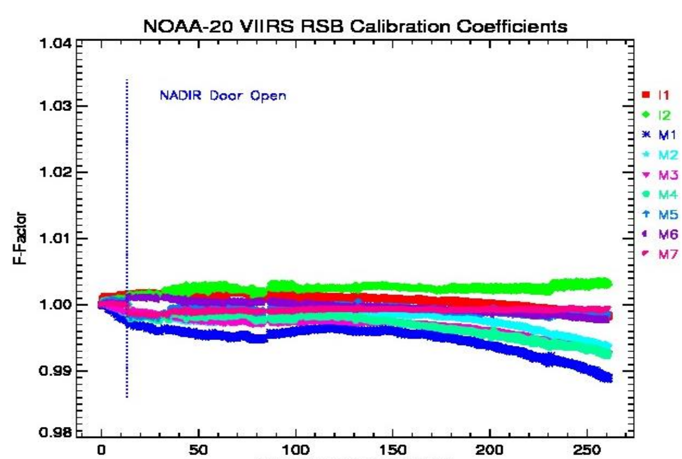

Figure 2. NOAA-20 VIIRS RSB calibration coefficients (or F-factors).

doi: 10.25923/w4k8-a710

While the derivation of the SD BRFs and SDS VF were standard, the SVS VFs turned out to be a familiar foe that was also the case for SNPP VIIRS and MODIS in their early mission. That is, the SVS VFs are very complex two-dimensional non-smooth functions and failed characterization by any reasonable smooth functions given the limited sets of yaw measurements. Here, we used an interpolated SVS VFs as a starting point for additional adjustment. The conventional approaches are to wait for additional SDSM measurements from routine operation requires up to one year of waiting period or to make an additional extended but costly yaw operation that still might still be insufficient. We developed a novel approach that achieved immediate calibration result with accuracy at the same level as that of the extended yaw or longer waiting period. The success of this approach arises from utilizing the local information that is already available within the data to make corrections directly in the H-factors for the impact of the inaccuracy from the interpolated SVS VFs. The details are fully described in [1].

The early mission H-factor results, corrected for the impact of the SVS VFs inaccuracy, are shown in Fig. 1. It is seen that the degradation is wavelength dependent, and the strongest effect occurs at the shortest wavelength. The overall early mission performance of the NOAA-20 VIIRS H-factors is expectedly very similar to that of the SNPP VIIRS [2].

The final F-factors, with H-factors applied to account for SD degradation, are shown in Fig. 2. Each point represents the directly computed outcome of an individual orbit without any averaging or smoothing scheme. Their smoothness and stability are indicative of the very good performance of the NOAA-20 VIIRS RSBs, and also showing surprisingly moderate gain changes at 1% or less over the initial 250 days. This gentle gain change is in stark contrast to SNPP VIIRS, which ran through as much as 25% over the same initial time interval [3]. Thus NOAA-20 VIIRS RSB is starting out to be a better performing instrument than SNPP VIIRS.

Although the instrument is shown to be operating well through F-factor performance, the F-factors are themselves not ready to be applied in the current form. SNPP VIIRS as well as the twin MODIS have been found to contain the a SD *degradation nonunifomity effect* (SDDNU) [2-5] that introduces long-term drift errors into the standard SD/SDSM calibration result and the associated science products. The NOAA-20 VIIRS, with its SD exhibiting the same overall behavior as that of SNPP VIIRS, thus is expected to have the same SDDNU effect that will also plague its RSB calibration result. Correcting for this error will require the incorporation of the lunar-based analysis, in the so-called "hybrid method" as is done for SNPP VIIRS [5], to generate the correct F-factors that can be applied to generate the correctly calibrated SDRs for NOAA-20 VIIRS.

References

1. J. Sun, M. Chu, and M. Wang, "On-orbit characterization of the VIIRS solar diffuser and attenuation screens for NOAA-20 using yaw measurements", *Appl. Opt*., 57, 6605-6619 (2018).
2. J. Sun and M. Wang, "Visible Infrared imaging radiometer suite solar diffuser calibration and its challenges using solar diffuser stability monitor", *Appl. Opt*., 53, 8571-8584 (2014).
3. J. Sun and M. Wang, "On-orbit calibration of the Visible Infrared Imaging Radiometer Suite reflective solar bands and its challenges using a solar diffuser," *Appl. Opt*., 54, 7210-7223 (2015).
4. J. Sun, M. Chu, and M. Wang, "Degradation nonuniformity in the solar diffuser bidiretional reflectance distribution function", *Appl. Opt*., 55, 6001-6016 (2016).
5. J. Sun and M. Wang, "Radiometric calibration of the Visible Infrared Imaging Radiometer Suite reflective solar bands with robust characterizations and hybrid calibration coefficients", *Appl. Opt.* **54**, 9331-9342 (2015).

Discuss the Article

doi: 10.25923/w4k8-a710

Improving S-NPP VIIRS Reflective Solar Band (RSB)Calibration Accuracy through Reprocessing

By Sirish Uprety (NOAA/UMD), Changyong Cao (NOAA), Xiaoxiong Xiong (NASA), Wenhui Wang (NOAA/ERT), Bin Zhang (NOAA/ERT), Taeyoung Choi (NOAA/ERT), Slawomir Blonski (NOAA/ERT) and Xi Shao (NOAA/UMD)

The Visible Infrared Imaging Radiometer Suite (VIIRS) onboard the Suomi National Polar-orbiting Partnership (S-NPP) satellite has gone through a number of major updates in the sensor data record (SDR) algorithm and calibration parameters over the mission life. This has led to temporal inconsistencies in the radiometric calibration of the NOAA operational S-NPP VIIRS SDR products. In order to make VIIRS data more useful and reliable for the scientific community, the entire VIIRS data record from January 2012 to March 2017 has been reprocessed. This version 1 reprocessing is complete and the SDR record is available to users upon request. The goal of this article is to provide a summary of version 1 and ongoing version 2 SDR reprocessing effort that uses a novel reprocessing technique.

Version 1 reprocessing uses RSBAutocal as a baseline calibration (onboard solar diffuser based) which is consistent with NOAA operational calibration. The VIIRS reflective solar bands (RSB) have undergone major operational calibration updates such as solar diffuser stability monitor (SDSM) screen transmittance tables update, prelaunch calibration coefficients update without an offset term (c0=0), optimized Robust Holt-Winters (RHW) filter parameters for SD degradation characterization, transition from manual F-factor (1/gain) computation to RSBAutoCal, solar vector error correction (Blonski & Cao, 2015). The F-factor is a multiplicative factor generated to compensate for the changes in instrument responsivity. The SDSM screen transmittance table update in early 2012 resulted in a nearly 2% improvement in radiometric accuracy for bands M1-M3. Similarly, update in prelaunch calibration coefficients with no offset term in April 2014 has improved the radiometric accuracy of solar bands with highest impact on band I3 by nearly 1%. This led to a consistent radiometric response between I3 and M10. An anomaly in SD degradation characterization in early 2014 led to optimization of RHW parameters in May 2014, which changed the radiance by nearly 2% for the blue bands. NOAA STAR has completed first set of reprocessing (version 1) that accommodates all the incremental updates to the operational SDR time series, leading to consistent radiometric calibration for the entire reprocessed time period. Version 1 reprocessed data also provides constant bias correction factors for M5 (1.5%) and M7 (2%). The bias correction factors are generated based on inter-comparison with AQUA MODIS and Landsat 8 OLI (Uprety et al., 2015).

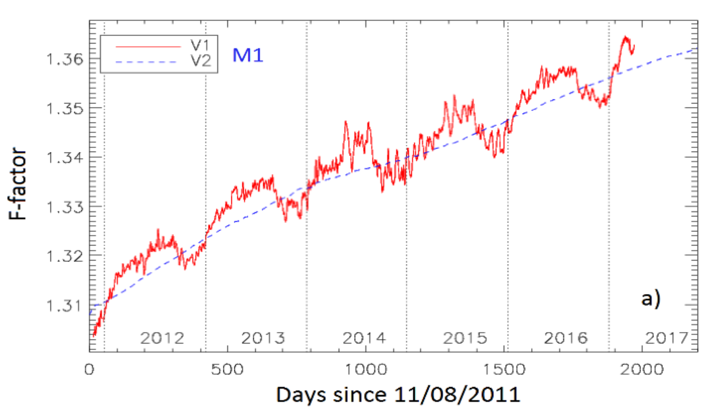

Figure. 1(a): RSBAutoCal V1 and V2 F-factors (M1),

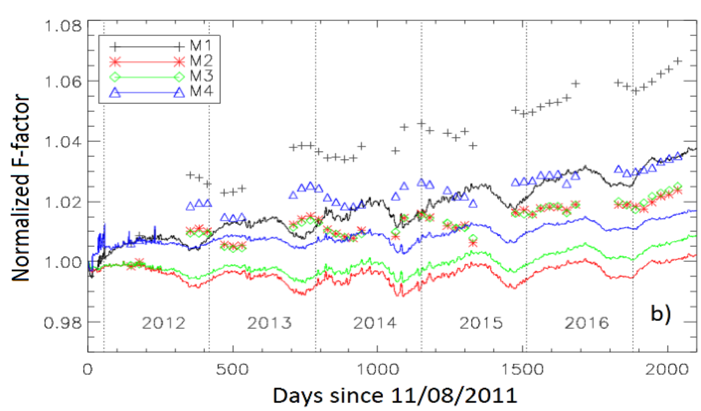

Figure. 1 (b): SD F-factor vs. GIRO Lunar F-factor

doi: 10.25923/w4k8-a710

In addition, users also have option to use the gain coefficients generated by the NOAA Ocean Color (OC) team, which are based on hybrid calibration of solar diffuser and moon (Sun and Wang, 2015). The bias correction table in each SDR data file contains the ratio of F-factors between RSBAutocal and OC. Users can convert to the OC version of reprocessed data by simply scaling the radiance with the given F-factor ratios.

OBC-based SD F-factors used in Version 1 reprocessing show annual oscillations (Figure 1a). Thus, S-NPP VIIRS yaw maneuver data were re-analyzed to derive improved SD and SDSM screen and BRDF LUTs for version 2 reprocessing. This leads to significantly reduced seasonal oscillation in the F-factors for short-wavelength bands. In addition, bands M1 through M4 in version 1 display time-dependent temporal bias (Figure 1b) on the order of 2% or less when RSBAutocal-based solar calibration F-factors are compared to lunar calibration F-factors.

To remove the long-term bias and further improve data quality in version 1 reprocessing, RSB calibration will be further enhanced in the upcoming version 2 reprocessing by using Kalman filter-based gain coefficients. The Kalman filter combines calibration results from latest SD-based solar calibration parameters with reduced oscillations, lunar, deep convective clouds, and extended simultaneous nadir overpass results. It also reconciles any discrepancies between low gain and high gain calibrations. Further, using DCC and SNO-x feedbacks provide an independent validation of SD and lunar-based instrument degradation characterization. Calculating the instrument degradation using multiple independent approaches and combining them for a best estimate of gain value resulted in optimal

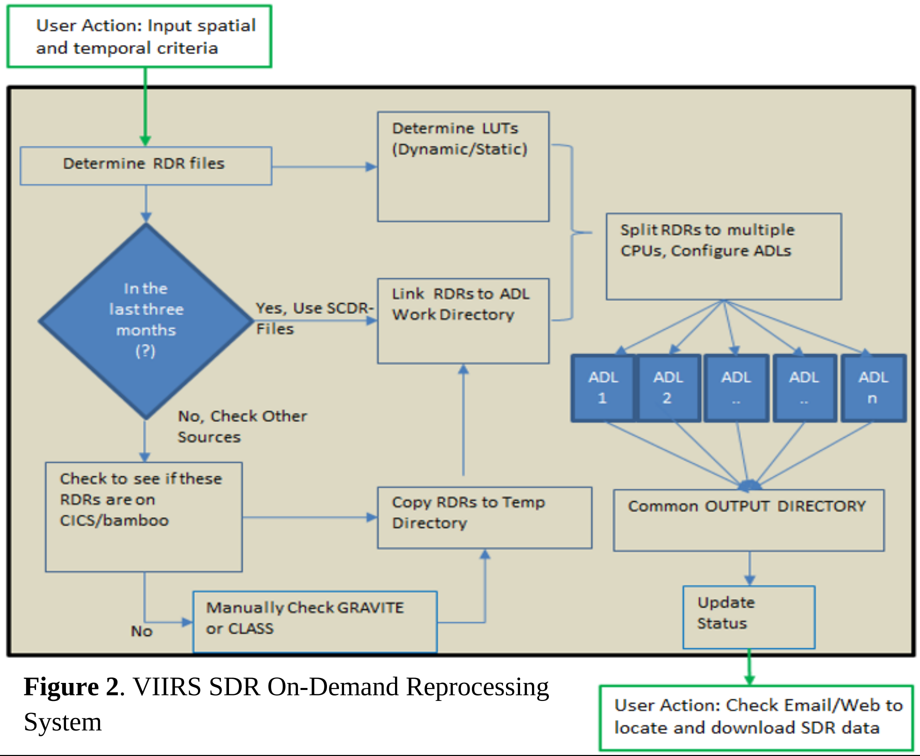

Figure 2. VIIRS SDR On-Demand Reprocessing System

calibration. This approach reduced uncertainties and bias associated with each technique by not relying on one particular method. It is to be noted that version 2 reprocessing uses Thuillier solar spectrum unlike the Kurucz spectrum used in version 1. This results in consistent solar model with NOAA-20 VIIRS.

In addition to radiometric improvements, optimal versions of geometric calibration LUTs are used in reprocessing to provide improved and consistent geometric accuracy. Short-term anomalies that exist in operational geolocation data before August 2013 are removed. The major updates were a) the initial instrument to spacecraft mounting matrix update on February 2012 which reduced I-band geolocation error from ~1 km down to ~24 m, b) the switch of scan control electronics (SCE) from Side-B to Side-A in November 2012, c) the star tracker maintenance/re-alignment in April 2013 and d) a final GEO PARAM LUT update in August 2013 (Wang et al., 2017). Reprocessed data have optimal geolocation accuracy with 3-sigma uncertainty better than 200 m.

To further facilitate the use of reprocessed VIIRS SDR data, version 2 reprocessing is being developed with the capability of On-Demand SDR reprocessing. This capability has been established for both S-NPP and NOAA-20 and its functionality has been successfully tested. Data storage and distribution are often the major challenges of reprocessing. With ~800 terabytes of SNPP VIIRS reprocessed SDR since launch, storage is a significant challenge for VIIRS reprocessing. Reprocessed output SDRs are nearly 10 times larger in storage than the input RDRs. Very often, data transmission such as through ftp is slower than data generation in reprocessing. Additionally, users can have their own specific needs regarding the spatial and/or temporal observations. The long-term goal is to store the reprocessed data in NOAA CLASS. Until then, reprocessing On-Demand is a strategy to address the above issues and can generate reprocessed SDR only upon the user request. In addition, it might be feasible

doi: 10.25923/w4k8-a710
GSICS Quarterly: Winter Issue 2018 Volume 12, No. 2, 2018

to generate SDRs at the users' site to reduce data transmission time. VIIRS SDR On-Demand reprocessing is performed using a wrapper that is being developed around ADL (Figure 2). This includes an interface design for user / administrator interaction, server configuration for parallel computing using limited resources, updating with latest look up tables, maintenance of the software errors, modifications and updates of ADL.

In conclusion, S-NPP VIIRS version 1 reprocessing is complete and available to users upon request. Meanwhile, a more robust VIIRS calibration approach using Kalman filtering is under development and will be implemented in upcoming version 2 reprocessing. In addition, On-Demand reprocessing has been established for version 2 to address the storage and distribution challenges of reprocessed VIIRS data. As expected, lessons learned from S-NPP will greatly benefit future data reprocessing for NOAA-20 VIIRS. The VIIRS SDR team looks forward to supporting the GSICS community with the best reprocessed VIIRS SDR data.

References:

Blonski, S., & Cao, C. (2015). Suomi NPP VIIRS Reflective Solar Bands Operational Calibration Reprocessing. *Remote Sensing*, *7*(12), 16131-16149.

Sun, J., & Wang, M. (2015). Radiometric calibration of the Visible Infrared Imaging Radiometer Suite reflective solar bands with robust characterizations and hybrid calibration coefficients. *Applied optics*, *54*(31), 9331-9342.

Uprety, S., and C. Cao. 2015. "Suomi NPP VIIRS Reflective Solar Band On-Orbit Radiometric Stability and Accuracy Assessment Using Desert and Antarctica Dome C Sites." Remote Sensing of Environment 166: 106–115. doi:10.1016/j.rse.2015.05.021.

Wang, W., Cao, C., Bai, Y., Blonski, S., & Schull, M. A. (2017). Assessment of the NOAA S-NPP VIIRS geolocation reprocessing improvements. *Remote Sensing*, *9*(10), 974, https://doi.org/10.3390/rs9100974.

Discuss the Article

COMS Visible Channel Calibration Using Moon Observation Data

by Tae-Hyeong Oh and Dohyeong Kim, KMA/NMSC

Through the use of the GSICS (Global Space-based Inter-Calibration System), the KMA (Korea Meteorological Administration) has monitored the radiometric performance of the COMS (Communication, Ocean and Meteorological Satellite) visible channel through its own calibration system and the use of four different Earth targets: ocean, desert, water cloud, and DCC (Deep Convective Cloud). To use the invariant target of the Moon, the KMA adopted GIRO (GSICS Implementation of the ROLO (Robotic Lunar Observatory) model), which was released by EUMETSAT.

.

Channel	Spectral Range (μm)	Central Wavelength (μm)	IFOV [1] (μrad)	Spatial Resolution (km)	Input Range	SNR [2] (VIS) and NEdT [3] (IR)
VIS	0.55–0.8	0.675	28 × 28	1	0–115% albedo	170:1 at 100% albedo
SWIR	3.5–4.0	3.75	112 × 112	4	4–330 K	0.10 K at 300 K
WV	6.5–7.0	6.75	112 × 112	4	4–330 K	0.12 K at 300 K
IR1	10.3–11.3	10.8	112 × 112	4	4–330 K	0.12 K at 300 K
IR2	11.5–12.5	12.0	112 × 112	4	4–350 K	0.20 K at 300 K

Table 1. Characteristics of COMS meteorological Imager

doi: 10.25923/w4k8-a710

Satellite	Time Coverage	Moon Observations (Times)	Channel	Absolute Phase Angle Range (Degree)		Useful Observation for Calibration	
COMS MI	Apr. 2011–Dec. 2017	152	Visible (0.6 μm)	0–90	0–30	146	60
					31–60		59
					61–90		27

Table 2. Characteristics of COMS MI Moon Observation Data.

To investigate degradation of COMS MI (Meteorological Imager) visible channel performance, several Moon observations (typically one per month) must be obtained with the following geometric and radiometric conditions to integrate the full signal produced by the Moon. First, the Moon image must be complete and include unilluminated regions; Second, there should be no interference in the Moon image from the Earth, the atmosphere, the Sun (no straylight), or from any star. As shown in Table 1, COMS observed the Moon 152 times from April 2011 to December 2017 (an average of twice a month). At least one Moon image acquisition per month is recommended. Of these observations, a total of 146 lunar observations were converted from Level 0- to Level 1A-equivalent data for COMS visible channel calibration. Level 1A is data radiometrically calibrated from raw data and is not geometrically corrected (no geolocation). Figure 1 shows the irradiance ratio (%) between instrument observations and the ROLO model of the COMS visible channel for a period of more than six years from April 2011 to March 2017. The long-term temporal trend clearly showed sensor degradation of about 8% throughout the total operational period. Lunar calibration results were compared with vicarious calibration results using DCC.

Figure 2 shows a comparison among degradation estimations from three calibration methods with respect to visible channel degradation of the COMS imager: Moon (orange dot), DCC (blue asterisk) and integrated method (green diamond) combining desert, ocean, and water cloud After selecting DCC targets, typical optical properties were assumed as inputs to the RTM (Radiative Transfer Model), based on an examination of DCC properties using MODIS cloud products. Reference values of sensor-reaching radiances were then produced from theoretical calculations, and these values were compared with Level 1B radiance products for calibration

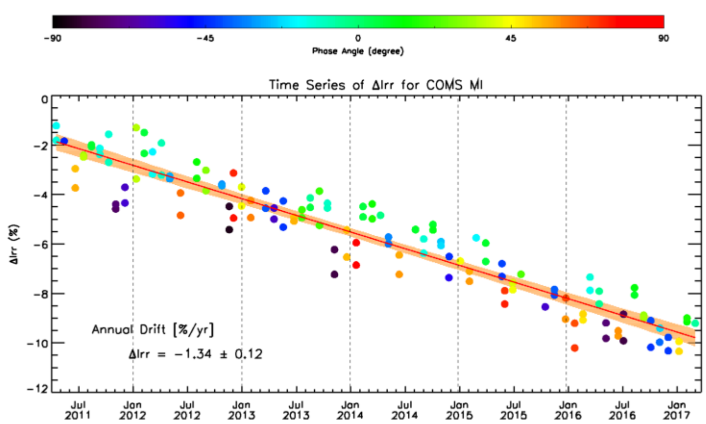

Figure 1. Temporal trend of COMS MI visible channel calibration from April 2011 to March 2017. Colors represent Moon phase angles and the orange shading represent the 95% confidence interval of the linear regression.

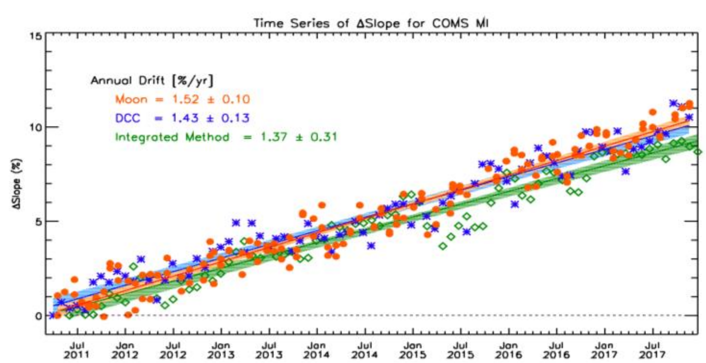

Figure 2. Comparison of visible channel degradation of COMS imager among several calibration methods: Moon (orange dot), DCC (using RTM) (blue asterisk) and integrated method (green diamond) from April 2011 to December 2017. The shadings represent the 95% confidence interval of the linear regression for moon (orange shade), DCC (light blue shade) and integrated method (green shade).

doi: 10.25923/w4k8-a710

monitoring. The bulk scattering properties for ice particles were used as a scattering database in the RTM. The two methods showed very similar annual drift values of 1.52 ± 0.10% per year and 1.43 ± 0.13% per year for Moon and DCC, respectively.
In addition to using the DCC method for comparison, three different earth targets were used (ocean, desert, and water cloud) to consider the wide reflectance range from the ocean's surface around longitude 70E–165E and latitude 30S–25N as well as from a water cloud around longitude128±40E and latitude 40S–40N. An integrated method combining desert, ocean, and water cloud showed a similar annual drift value of 1.37 ± 0.31% per year. The irradiance ratio between GIRO and lunar observations showed strong seasonal variation due to seasonal variation in the phase angle of the Moon. Furthermore, the phase angle of the Moon showed a similar pattern every half year, which was related to Moon observation attitude and time. Phase angle dependence was corrected to remove seasonal variation of Moon irradiance. After angle correction was applied, the annual drift value remained the same but the standard deviation was reduced from 0.78 to 0.51.
This study reports the long-term characteristics of the COMS MI visible channel for the first time through the application of GSICS concepts, implementation of GIRO, and the use of moon observation data from April 2011 to December 2017. Results indicated that the irradiance ratio between GIRO and lunar observations of COMS MI showed strong seasonal variation due to seasonal variation in the phase angle of the Moon.

Long-term monitoring of COMS MI visible channel calibration was conducted by using Moon observation data from April 2011 to December 2017 under GSICS frameworks. The annual drift estimate using Moon observations and the GIRO model was 1.52 ± 0.10% per year; this value is comparable with that of the DCC and integration methods (i.e., 1.43 ± 0.13% per year and 1.37 ± 0.31% per year, respectively). Notably, the lunar calibration result was in good agreement with that provided by vicarious calibration, such as the DCC and integration methods. This appears reasonable with respect to the relatively broad range of annual drift values, as the expected drifts were between one and several percent over five years, despite the very stable design of the imaging instrument.

References

Kieffer, H.H.; Stone, T.C. The spectral irradiance of the Moon. *Astron. J.* 2005, *129*, 2887–2901.

Stone, T.C.; Kieffer, H.H.; Anderson, J.M. Status of Use of Lunar Irradiance for On-orbit Calibration. *Proc. SPIE* 2002, *4483*, 165–175.

Doelling, D.; Morstd, D.; Bhatt, R.; Scarino, B. Algorithm Theoretical Basis Document (ATBD) for Deep Convective Cloud (DCC), 2011. Available online: https://gsics.nesdis.noaa.gov/pub/Development/AtbdCentral/GSICS_ATBD_DCC_NASA_2011_09.pdf (accessed on 02 May 2016).

EUMETSAT, High Level Description of the GIRO Application and Definition of the Input/Output Formats, 2015. Available online: http://gsics.atmos.umd.edu/bin/view/Development/LunarWorkArea (accessed on 02 February 2015

Discuss the Article

Assessment of Microwave Radiometers On-board Altimetry Missions: Comparison of measured brightness temperatures to simulations

by Bruno Picard, Marie-Laure Frery and Mathilde Siméon (CLS, France)

Since 1992, altimetry missions aim at measuring the sea surface topography with an uncertainty better than 1 cm over a grid mesh and the global mean sea level rise (established at +3 mm/year over the altimetry era) with an uncertainty less than 0.3 mm/year over a decade (GCOS recommendations for Sea Level). The wet tropospheric correction (WTC) accounts for the path delay on the radar signal due to the water vapor. It is a major source of uncertainty on the altimetry budget error, due to its large spatial and temporal variability. It also contributes significantly to the uncertainty in the long term mean sea level trend.

In order to fulfill these strong constraints on uncertainties, microwave radiometers are usual companions to the main radar instrument on altimetry missions, dedicated to the retrieval of the WTC in exact coincidence with the altimeter range measurement. Different observation frequencies are used, as the three channel configurations (18.7 GHz, 23.8 GHz, 31.4 GHz) for AMR on-board Jason-3 mission (CNES, NASA, EUMETSAT, NOAA) or two channel configurations (23.8 GHz, 36.5 GHz) for MWR on-board Sentinel-3 A/B (ESA, EUMETSAT) or

doi: 10.25923/w4k8-a710

SARAL/AltiKa (CNES, ISRO).

The WTC is retrieved by using empirical approaches, a log-based stratified algorithm on Jason's series (JPL) [1], a neural network on Sentinel-3 series and SARAL/AltiKa (CLS) [2]. As for any empirical approach, any modification of the statistics of the measured brightness temperatures (drops, jumps, drift) has an impact on the WTC: a rule of a thumb states that a 1 K error on the 23.8 GHz leads to a 5 mm error on the WTC. Since any error on the WTC retrieval has a direct impact on the topography the monitoring of the radiometer, Tb is critical. In addition to a large panel of metrics dedicated to the assessment of Tb (geographical selection of hottest Tb over the Amazonian forest, statistical selection of the coldest Tb over ocean), a systematic comparison to simulated Tb is also applied.

The 6-hourly ECMWF global analysis are extracted every day on a 0.25°x0.25° Cartesian grid. Atmospheric profiles and surface conditions are the main inputs to the CLS/IPSL/UCL radiative transfer model. Close to NWP SAF RTTOV, the CIU model is based on the Boukabara double-scale emissivity model associated with the Elfouhaily directional spectrum for the sea surface roughness; the Liebe-93 MPM is used for the gaseous absorption of oxygen and water vapor in the atmosphere. In order to limit the computation time, the first step consists on a selection of the ECMWF grid cells where MWR observations occur within ±30-minutes from the analysis time. For each of the selected cells, the ICU model is applied, and the simulated Tb is associated to each observation lying in the cell. Figure 1 shows the monitoring of the weekly averages of the difference between observed and simulated Tb. A 11-days Savitzky-Golay filter is applied to remove the high frequency variations. The time series are plotted for four different instruments (SARAL/AltiKa MWR in blue, Metop-A/AMSU-A in red, Sentinel-3 MWR in green and Jason-3 AMR in purple), for the 23.8 GHz channel on the left panel and for the liquid water channel on the right panel (there are small differences on the central frequencies depending on the instrument) and split between descending half-orbits (dark colors) and ascending half-orbits (light colors). We are focusing on the common period of Sentinel-3A and Jason-3, since March 2016 up to May 2018. It's worth noting that AMSU-A being a sounder, a "nadir" observation is artificially computed from the linear interpolation between the two closest pixels from the satellite nadir.

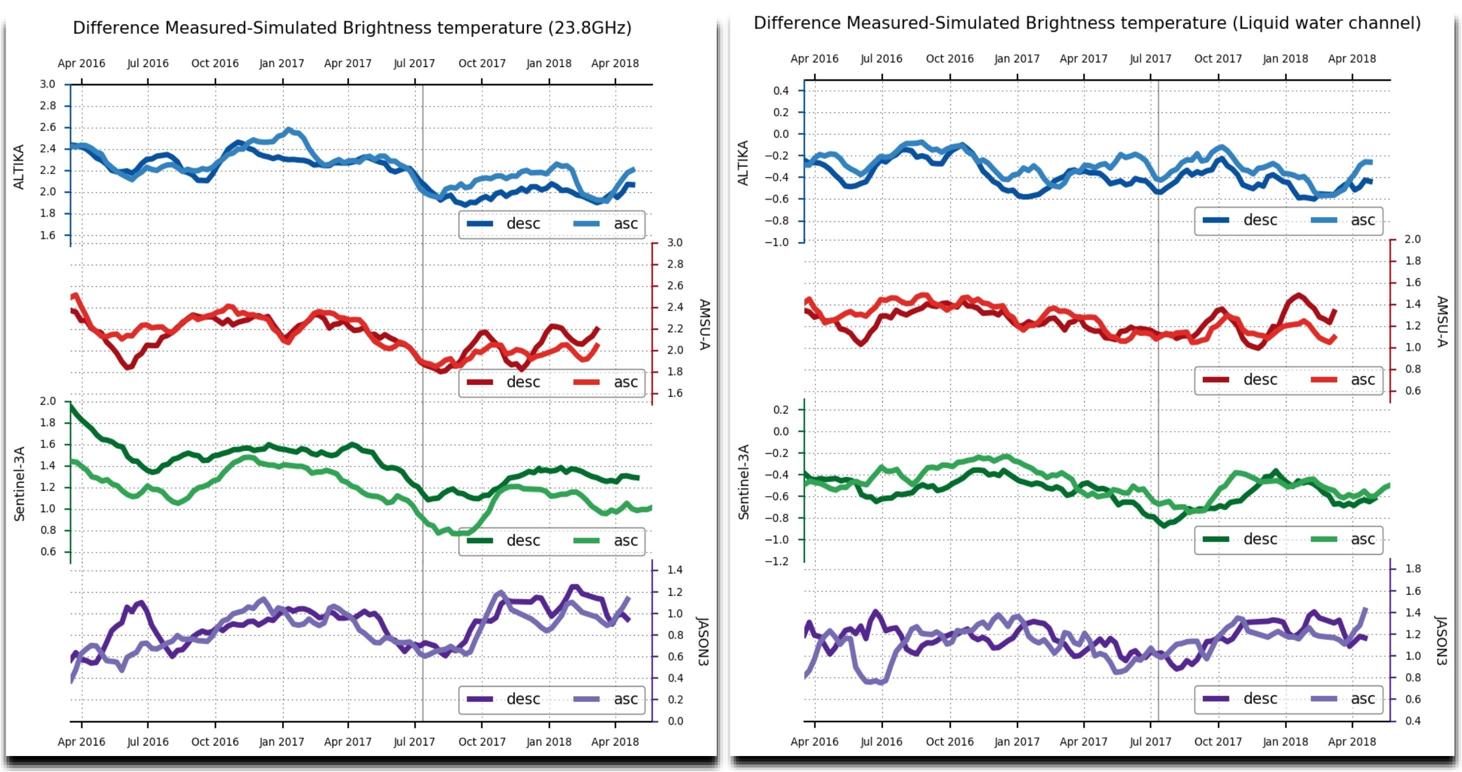

Figure 1: Monitoring of the weekly averages of the difference between observed and simulated Tb.

doi: 10.25923/w4k8-a710

For a given instrument and a given channel, the amplitude of the bias is explained by the properties of the ICU model, the version of the ECMWF IFS system and by the instrumental properties, mainly the in-flight calibration choices made by the team responsible for this particular instrument. Then, any variation in the difference can be attributed to any of these components.

After July 2017, the average bias on the 23.8 GHz seems to be lower than before, at least for AltiKa, Sentinel-3 and AMSU-A. So, the reason is not related to an instrument issue. It could be attributed to an inter-annual variability of the atmosphere but, since it coincides with the CY43R3 version change of ECMWF IFS that occurred on 2017, July 11th (clearer on the non-filtered time series), it is more likely due to the evolution of the model. The impact on Jason-3 is negligible but it may be due to the fact that it belongs to the only non-synchronous orbit mission amongst the four instruments: a complete year would be needed to draw more robust conclusions.

Such an approach also allows one to detect fine instrumental impact on the observations. The 23.8 GHz channel of Sentinel-3 MWR exhibits a bias of about +0.3 K between ascending and descending pass which cannot be detected in the monitoring of AltiKa and AMSU-A (Jason-3 split between ascending and descending half-orbit is not representative of a day/night discrimination). The specific accommodation of the reflector with respect to the platform is suspected to be the source this bias, which would also explain why the bias is not so obvious on the 36.5 GHz channel. The 23.8 GHz channel antenna pattern being wider than the 36.5 GHz channel, it may happen that an undesirable signal reflected by the platform impacts the observed Tb. Even though the final impact on the WTC is very low, of the order of 1 mm, so the quality of Sentinel-3 altimeter budget error is not affected, a study is on-going, funded by ESA/ESTEC, which aims at characterizing this signal and proposing a potential correction.

In conclusion, the comparison between observed and simulated Tb is confirmed to be a metric particularly adapted to the assessment of the stability of microwave radiometers, especially when monitoring various instruments simultaneously.

Acknowledgment: this activity is supported by CNES SALP and ESA/EUMETSAT MPC projects.

References

[1] S. Brown, "A novel near-land radiometer wet path-delay retrieval algorithm: Application to the Jason-2/OSTM Advanced Microwave Radiometer," IEEE Trans. Geosci. Remote Sens., vol. 48, no. 4 PART 2, pp. 1986–1992, 2010, DOI:10.1109/TGRS.2009.2037220

[2] B. Picard, M.-L. Frery, E. Obligis, L. Eymard, N. Steunou, and N. Picot, "SARAL/AltiKa Wet Tropospheric Correction: In-Flight Calibration, Retrieval Strategies and Performances," Mar. Geod., vol. 38, 2015, DOI:10.1080/01490419.2015.1040903

Discuss the Article

News in this Quarter

GSICS 19th Executive Panel Meeting (EP-19) held in Bangalore, India

by Mitch Goldberg (NOAA), Kenneth Holmlund (EUMETSAT), Toshi Kurino (WMO), Lawrence Flynn (NOAA), Manik Bali (NOAA), Dohyeong Kim (KMA) and Masaya Takahashi (JMA)

Prior to the CGMS-46 meeting, the GSICS Executive Panel (EP) Members from CMA, EUMETSAT, ISRO, JAXA, JMA, KMA, NASA, NOAA, ROSHYDROMET, ROSCOSMOS along with WMO Secretariat (Toshiyuki Kurino), GSICS Coordination Center Deputy and CGMS SWTT Chair, convened for the Annual GSICS EP meeting on 1-2 June 2018.

On the agenda were key decisions, endorsements and guidance from the EP on topics related to in-orbit monitoring of meteorological satellites by member agencies. Some of the items that were reported are described below.

GSICS Coordination Center (GCC) Deputy Director, Manik Bali (NOAA Affiliate UMD), gave an overview of the progress made by the GCC in meeting the needs of the GSICS community. Among the highlights were the following: 1) GCC facilitated the acceptance of seven new products into the GSICS Product Catalog. Manik thanked the reviewers of the products, Chairs, Co-Chairs of Groups and the EP for their role in the acceptance process.

doi: 10.25923/w4k8-a710

Participants in the GSICS EP-19 meeting

Products include those using IASI-A, AIRS and IASI-B as references in Near Real Time and Re-Analysis mode. 2) Continued development of the Action Tracker on the Google Cloud has led to a reduced overhead. And 3) The GSICS newsletter membership around the world increased to 344 persons. He also thanked ROSHYDROMET for their support in organizing the GSICS session in the AOMSUC held in Vladivostok, Russia.

Doheyong Kim, Chair GSICS Research Working Group (GRWG) gave a summary of GRWG activities in the UV, MW, IR and VIS subgroups. He began by reporting on calibration results of next generation satellites. This included FY-4A satellite (GIIRS, AGRI and LMI), GOES-16 and CrIS and VIIRS on NOAA-20 as well as SNPP. Advances in SRF retrieval method, Spectral Gap filling, MTF, and cross-talk characterization were reported to EP.

For the UV subgroup, there was progress on comparisons of solar measurement from backscatter ultraviolet instruments and on the white paper on ground-based characterization of UV spectrometers.

Doheyong also reported on the SCOPE-CM IOGEO (SCM-06 IOGEO) activity and its plans to align with the GSICS. Doheyong gave a breakdown of the consistent support of member agencies towards meeting GSICS goals and objectives. The IR subgroup designated IASI-A and SNPP-CrIS as in-orbit GSICS references.

For the VIS/NIR subgroup, Doheyong reported that SNPP-VIIRS has been accepted as the GSICS VIS reference and will provide continuity to MODIS instruments that have been the mainstay of in-orbit reference in GSICS. He also stated that the CLARREO team would seek inputs from GSICS and priorities on which geostationary satellites and invariant targets to characterize spectrally. The VIS/NIR subgroup also conducted a successful 2nd GSICS-IVOS Lunar Calibration Workshop in Xian in China. He reported that GIRO/GLOD license agreement have been recently signed by JMA, USGS, KMA, JAXA, CNES, ESA. The distribution of the GIRO code has started for those agencies. But the GLOD will be provided at a later stage once it is consolidated

In the Microwave subgroup Doheyong highlighted the recent advances in identifying in-orbit reference records for monitoring Microwave instruments and the best practices for MW instrument monitoring. The Microwave subgrouo is working closely with CEOS-IR, GRUAN and GPM-X to fulfill the needs of WIGOS observing system

Masaya Takahashi (GDWG Chair) provided the EP updates on three important tasks undertaken during the past year. First is the establishment of

doi: 10.25923/w4k8-a710

collaboration servers that host and share GSICS Deliverables (e.g. GSICS Corrections) in CMA, NOAA and EUMETSAT. ISRO has established a thredds server that is expected to be integrated into the collaboration server architecture. Second is GSICS Plotting tool that plots the GSICS products an upgrade is underway at EUMETSAT. Third is future activities on Satellite Instrument Event Logging, which were agreed upon among GSICS member agencies. The GDWG Chair also presented the report on State of Observing System which summaries the monitoring of instruments of member agencies along with relevant uncertainties. A follow up report on this was presented at the CGMS by the GSICS EP.

Kennneth Holmlund reviewed the status of the GSICS Procedure for Product Acceptance (GPPA). Ken's discussions with GCC (Manik Bali) generated actions to reduce timeliness in product acceptance and promotion of products in maturity.

The executive panel decided to invite the European Space Agency, to become a full member of the GSICS Executive Panel. It also decided to discuss with the Space Weather Community whether it would make sense to be a part of the GSICS.

Overall, nineteen Actions and two Recommendations were generated in this EP meeting. A detailed EP-19 report has been uploaded at http://www.wmo.int/pages/prog/sat/meetings/GSICS-EP-19/GSICS-EP-19.html

Discuss the Article

GSICS and GRUAN Coordination: RIVAL to the Rescue?

by Tony Reale (NOAA) and Lori Borg (SSEC, Univ. Wisconsin)

A concerted effort to utilize Global Climate Observing System (GCOS) Reference Upper Air Network (GRUAN) to supplement GSICS in the monitoring and assessment of environmental satellite sensors including CrIS, IASI, HIRS, ATMS and AMSU https://www.wmo-sat.info/oscar/instruments was initiated at the GSICS Annual meeting in 2017 (see GSICS Quarterly, Winter 2018).

Figure Above: RIVAL dual launch of Vaisala RS92 and RS41 radiosondes synchronized with NOAA-20 polar satellite overpass at the DOE-ARM Eastern North Atlantic (ENA) Azores site. *(Courtesy Donna Holdridge, Argonne National Laboratory)*

A labor intensive component of this effort has been the access and appending of the Sensor Data Records (SDR) to the benchmark collocations of GRUAN radiosondes and atmospheric sounding Environmental Data Records (EDR) stored in the NOAA Products Validation System (NPROVS) for the multiple satellites of interest (to GSICS). Preliminary results from long-term studies of radiosonde (RAOB)-satellite Microwave and GPSRO trend consistency (by Bomin Sun (STAR-IMSG), Cheng-zhi Zou (STAR) and Johannes Nielsen (DMI)) and also on the consistency of calculated infra-red sensors (LBL) from RAOB and NWP -satellite observations (by Bomin Sun (STAR-IMSG), Xavier Calbet (AEMET) and Manik Bali (STAR-UMD)) have emerged and are promising. Nevertheless, overall progress is slow as resources are tight.

However, activities to leverage the Radiosonde Inter-comparison and VALidation (RIVAL) program in support of GSICS/GRUAN objectives are underway. RIVAL is a joint proposal sponsored by ARM and coordinated among NOAA STAR and manage the transition from Vaisala RS92 to RS41 radiosondes mandated

doi: 10.25923/w4k8-a710

by Vaisala Corporation's decision to cease production of the RS92 in lieu of the RS41 beginning in September, 2017. The Vaisala RS92 has been the standard radiosonde flown at ARM since 2005 and has served as the reference radiosonde flown at GRUAN sites since 2008. RIVAL is a proposed 2-year program to routinely launch concurrent (Dual) RS92 and RS41 radiosondes that are targeted for NOAA-20 satellite overpass; S-NPP satellite overpass is typically 50 minutes prior to NOAA-20. The plan is to provide a RIVAL dual-launches weekly at each of the ARM/GRUAN sites at South Great Plains (SGP), Oklahoma, North Slope, Alaska (NSA), Point Barrow and Eastern North Atlantic (ENA), Azores. Two types of launch configurations are planned. The first configuration consists of a dual launch about 45 minutes prior to overpass followed by a single RS41 launch about 5 minutes prior to overpass. This configuration will be used at SGP and at NSA. The second configuration is comprised of a single, dual launch about 15 minutes prior to overpass. Only single, dual launches are done at ENA due to site limitations.

RIVAL was accepted by ARM for year-1 with plans for a follow-up year-2 which is currently under review. The first RIVAL launches at SGP occurred on February 13 and at ENA and NSA on April 26 and June 20, respectively. As of August 18, twenty RIVAL launches (19 of them dual followed by single) have occurred at SGP, two (one a dual followed by single) at NSA and eleven at ENA. A predominance of cloudy sky weather conditions and wind at NSA has compromised the launch frequency and is being addressed. Staff at the respective sites are instructed not to launch in predominantly overcast, precipitating or windy conditions (and at NSA in presence of polar bears).

So how is RIVAL bridging GRUAN and GSICS? Among the objectives for RIVAL, perpetuated by GRUAN, was the inclusion of satellite based SDRs to analyze the RS92 to RS41 transition in the radiance as well as the geophysical space. Previously (since 2012), the primary objective of the JPSS program was the validation of sounding EDR and associated algorithm development support using the JPSS funded dedicated radiosondes at ARM sites synchronized with NOAA polar satellite overpass. The timing of RIVAL coincided with both the RS92 to RS41 transition period and the operational deployment of NOAA-20, the latter fueling justification for the inclusion of the SDR (along with EDR) within this unique RIVAL collocation dataset. Although the EDR is the single closest sounding to the radiosonde(s), the SDR (identified using the EDR) would span a 500km radius centered at the radiosonde location. Once compiled and certified, these dataset will be made available to the global community.

Another stipulation for the RIVAL collocation dataset is the additional targeting of pending COSMIC-2 GPSRO observations during 2019; COSMIC-2 is tentatively scheduled for deployment no earlier than December, 2018. This would require that predicted COSMIC-2 observations at each ARM site be received by the RIVAL launch scheduling group two weeks in advance. These data are also desired within the overall COSMIC-2 validation program being conducted jointly by UCAR and NOAA.

Work is underway to use RIVAL collocations to support ongoing analysis on the utility of GRUAN to monitor the ATMS sensor SDRs and TDRs (personal communication, Isaac Moradi, Univ Md, CICS). Follow-up work to use these data to analyze the utility of GRUAN to monitor CrIS (infrared) is anticipated. These are focused on targeted GRUAN collocation with NOAA-20 but also include S-NPP (50 minutes earlier) of values to analyze impacts due to spatial/temporal mismatch. These assessments will nicely compliment the primary objective of RIVAL to support the management of the RS92 to RS41 transition at ARM and GRUAN sites (and globally).

Finally, and of direct interest to GSICS researchers and developers, is the likelihood of RIVAL observations that include CFH advanced moisture radiosondes targeted for MetOp (IASI, AMSU), possibly MetOp-C tentatively scheduled for launch November, 2018. Stay tuned.

Discuss the Article

doi: 10.25923/w4k8-a710

Announcements

ROSCOSMOS joins as full member of GSICS Executive Panel

by Mitch Goldberg (NOAA), Toshi Kurino (WMO) and Lawrence Flynn (NOAA)

The GSICS Executive Panel is pleased to welcome ROSCOSMOS as a full member of the GSICS Executive Panel.

Over the years, ROSCOSMOS and ROSHYDROMET have made critical contributions to GSICS. Following their inclusion in the GSICS Executive Panel, ROSCOSMOS and ROSHYDROMET sponsored a GSICS Session in the AOMSUC-8 held in Vladivostok from 18-21 Oct 2017. Alexey Rublev (ROSHYDROMET) edited a special issue of the GSICS Quarterly Newsletter Issue, Summer 2018, earlier this year that focused on inter-calibration research in Russia providing further coverage of their latest advances in the development and applications of calibration methods

With the inclusion of ROSCOSMOS we expect to have enhanced collaboration among GSICS members.

GSICS Annual Meeting to be held at ESA in Frascati, Italy

by Philippe Goryl, ESA

The 2019 GSICS Joint Meeting on Research and Data Working Groups will be hosted by ESRIN, European Space Agency. The venue is ESA / ESRIN in Frascati, Italy. Dates would be finalized in due course.

The meeting will begin with a Mini-Conference, which is a session to discuss and introduce GSICS products and items that are not yet directly linked to existing GSICS Products. This will be followed by a Plenary. The plenary is a member oriented session and will cover topics related to the UV-VISNIR-IR-MW subgroups of GRWG and to activities of the GDWG and GCC. Reports from GSICS Processing and Research Centers (GPRCs) and discussion on cross-cutting issues will also be included. Following this, the GSICS Data Working Group (GDWG) and the GSICS Research Working Group (GRWG) will break out into parallel sessions while converging on important topics. The meeting will finish with a wrap up session where participants will discuss a summary of the meeting and the status of action items. Details of the meeting will be announced through the GSICS Wiki.
http://gsics.atmos.umd.edu/bin/view/Development/AnnualMeeting2019

GSICS-Related Publications

Oh, T.-H., and D. Kim. 2018. 'COMS Visible Channel Calibration Using Moon Observation Data'. *Remote Sensing* 10 (5). https://doi.org/10.3390/rs10050726.

Chen, R. 2018. 'Creating a Consistent Oceanic Multi-Decadal Intercalibrated TMI- GMI Constellation Data Record'. PhD Thesis, University of Central Florida. http://stars.library.ucf.edu/cgi/viewcontent.cgi?article=6816&context=etd.

Datta, Saswati, W. Linwood Jones, and Ruiyao Chen. 2018. 'Identifying Desert Regions for Improved Intercalibration of Satellite Microwave Radiometers'. *IEEE Journal of Selected Topics in Applied Earth Observations and Remote Sensing* 11 (6): 1895–1904. https://doi.org/10.1109/JSTARS.2018.2796184.

Li, Wen-Xia, Geng-Ming Jiang, Guicai Li, and Chuan Li. 2018. 'Intercalibration of Advanced Himawari Imager's Infrared Channels with IASI/Metop-B 1C Data'. *IEEE Journal of Selected Topics in Applied Earth Observations and Remote Sensing* 11 (6): 1989–96. https://doi.org/10.1109/JSTARS.2018.2801305.

doi: 10.25923/w4k8-a710

Submitting Articles to GSICS Quarterly Newsletter:

The GSICS Quarterly Press Crew is looking for short articles (800 to 900 words with one or two key, simple illustrations), especially related to calibration / validation capabilities and how they have been used to positively impact weather and climate products. Unsolicited articles may be submitted for consideration anytime, and if accepted, will be published in the next available newsletter issue after approval/editing. Please send articles to manik.bali@noaa.gov.

With Help from our friends:

The GSICS Quarterly Editor would like to thank Tim Hewison (EUMETSAT), Sriharsha Madhavan (SSAI) and Lawrence E. Flynn (NOAA) for reviewing articles in this issue.

Published By

GSICS Coordination Center
NOAA/NESDIS/STAR NOAA
Center for Weather and Climate Prediction,
5830 University Research Court
College Park, MD 20740, USA